Kem eKids

330 E 700 N

Provo, UT 84606

April 14, 2016

Dr. John Hedengren

350 CB Brigham Young University

Provo, UT 84606

Dr. Hedengren:

Power generation utilizing renewable energies is a growing part of the energy portfolio, yet it suffers from several drawbacks. One of the main drawbacks stems from the intermittency of renewable energy sources, such as wind and solar. When such renewable energy sources are not available, a plant still needs to reliably produce power. Building traditional fossil fuel power plants alongside renewable energy plants is expensive and a poor use of capital. However, hybridization of renewable energy and fossil fuel plants shows promise. This work simulates a power plant which uses solar thermal energy combined with a Brayton cycle power generation system. This combination increases the cycle time, allowing the plant to meet necessary power demand.

Another unique feature of this hybrid system is the addition of thermal energy storage into the simulation. The storage provides a heat sink for incoming air, leveling solar contributions in the day and utilizing them at night. These simulations provide useful data on the impact hybrid systems could have in the future.

Respectfully,

Anthony Bennett

Nathaniel Gates

Darrik Miller

Optimization and Control of a Hybrid Power Generation System

Authors

Anthony Bennett

Nathaniel Gates

Darrik Miller

Kody Powell

Abstract

Increasing energy demands and the need to decrease greenhouse gas emissions has driven power producing companies toward utilizing renewable energy sources. One of the main drawbacks in utilizing renewable energy is the intermittency of the power source. In an attempt to overcome these limitations, this paper simulates a combined thermal energy and Brayton cycle to meet energy demands. By using the combined cycle, many of the drawbacks of relying solely on renewable energies to meet power demand can be met. The hybrid system responds to changing energy demands while minimizing the use of fossil fuels.

- Simulation of hybridized power plant system
- Simulation of an energy storage system
- Model predictive control designed to meet power demand and minimize fuel usage
- Groundwork for future hybridized power plant systems

Introduction

Fossil fuels have supplied the world's energy needs for many years. Recent concerns about the environmental impact and the effect on climate has generated interest in other energy sources that are carbon neutral, as well as renewable. Solar radiation is one such technology, and is desirable because of the essentially limitless supply of energy radiating from the sun to the earth. However, the inherent intermittency in using solar energy for electrical generation remains a drawback to making it a reliable source of energy. In addition, the high-cost of solar compared with fossil fuels makes solar difficult to justify. One area of research that aims to overcome these challenges is power production hybridization, combining fossil fuels and renewable energy to provide a reliable source of power. Combining these two technologies will enable solar power to be utilized at a lower cost, as well as increasing the capacity factor of the plant. In addition, thermal energy storage can be used to maximize the amount of power generated from solar energy and minimize the required amount of fossil fuels. The purpose of this project is to simulate and optimize such a hybrid system, incorporating solar radiation with the Brayton cycle, and utilizing thermal energy storage in order to reliably generate electricity at a substantially lower cost than with solar radiation alone.

Literature Review

Modeling and optimization of systems utilizing solar radiation in combination with thermal energy storage is an on-going area of research [1-5]. Use of an energy storage system enhances the reliability of solar power, increasing the solar power capacity by as much as 47% [3-5]. It

was also found that empirical correlations for heat transfer in packed bed reactors have previously been simulated [6]. These correlations are used in the model simulation in this report. Electrical generation via the Brayton cycle has also been optimized using model predictive control, with real-time implementation increasing a plant's ability to respond to changes in electricity demand [1]. The model predictive control was found to have better responses to changes in power output with lower settling times and less oscillatory behavior than a typical PID controller. Implementing a feed forward controller feeding in weather forecasts has also been accomplished but not implemented in this simulation [2]. This implementation is discussed in the future work section.

Model Description

The objective of this process is to generate the required power using a solar radiation system in combination with the Brayton cycle, while incorporating thermal energy storage to enable load-shifting. First and foremost, the energy output of the plant must match the energy demand. Additionally, it is desired to maximize the amount of solar energy captured and minimize the amount of natural gas used. Finally, the plant's efficiency should be as high as possible.

The process works by pulling in air through a compressor and pressurizing it to 10-15 atm. Inlet guide vanes (IGV) are angled to control the amount of air pulled in at any given time and ultimately influence the amount of power generated. The air is then sent to a solar receiver, where a field of mirrors concentrate sunlight to a focal point, heating the air up to 1100 °C. The air then travels to a thermal energy storage unit, where it either stores or receives energy. After this, the air is heated up with a combustor fueled by natural gas. The air then travels through a turbine, generating electricity. A heat recovery steam generator (HRSG) captures the remaining energy from the air by using it to heat up steam. The air exits at approximately 200 °C, and the steam travels through a steam turbine, generating more electricity. A complete diagram of the model can be found in the appendix.

Model Optimization Variables

The manipulated variables that influence the dynamics of the system are:

- Inlet Guide Vane (IGV) angle (controls airflow amount)
- Natural gas flow to the combustors

The manipulated variables will change over the time horizon due to variable power output requirements. The power output requirements depend on consumer demand that varies throughout the day and week. This results in the need for the manipulated variables to change with time.

Thermal Energy Storage Model

A key component of this project is to model the storage of thermal energy. The storage unit is comprised of a cylindrical tank filled with cement spheres of 15 cm diameter. The heat transfer through the system is approximated as 1-D and discretized throughout the length of the tank. The correlations used to model the tank are shown below.

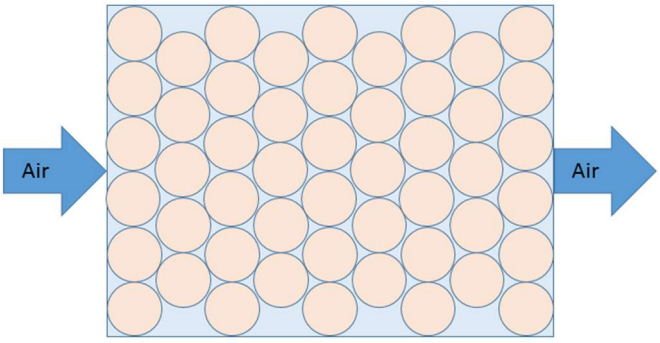

Figure 1: Thermal energy storage system

Heat Transfer

Conduction
$$q_{cond_i} = \frac{k_{stone}\, A_c}{x} \left(T_{stone_i} - T_{stone_{i+1}}\right) \quad (1)$$

Convection
$$q_{conv_i} = h * SA \left(T_{air_i} - T_{stone_i}\right) \quad (2)$$

Radiation
$$q_{rad_i} = \epsilon\, \sigma\, SA \left(T_{air_i}^4 - T_{stone_i}^4\right) \quad (3)$$

Energy Balance

Stone
$$m_{stone_i}\, Cp_{stone_i} \frac{dT_{stone_i}}{dt} = q_{conv_i} + q_{cond_i} - q_{cond_{i-1}} + q_{rad_i} \quad (4)$$

Air
$$m_{air_i}\, Cp_{air_i} \frac{dT_{air_i}}{dt} = m_{air.in}\, Cp_{air_{i-1}} \left(T_{air_{i-1}} - T_{ref}\right) \quad (5)$$

$$- m_{air.in}\, Cp_{air_i} \left(T_{air_i} - T_{ref}\right) - q_{conv_i} - q_{rad_i}$$

Model Predictive Control

The model predictive control utilizes the first principles equations found in the model. The model predictive control has the following inputs: total power, firing temperature, exhaust temperature air flow rate and the power setpoint. The power setpoint is set as a deadband for the power setpoint. To keep the controller above the setpoint, a large penalty is placed in the model for going below the lower power setpoint. This is similar to reality where power plants are fined for not producing the required power output. Costs are also added for using fuel and air, with the fuel cost being higher. This helps the optimizer minimize the use of fuel when possible. The firing temperature also has an upper limit to reduce side reactions and ultimately harmful pollutants.

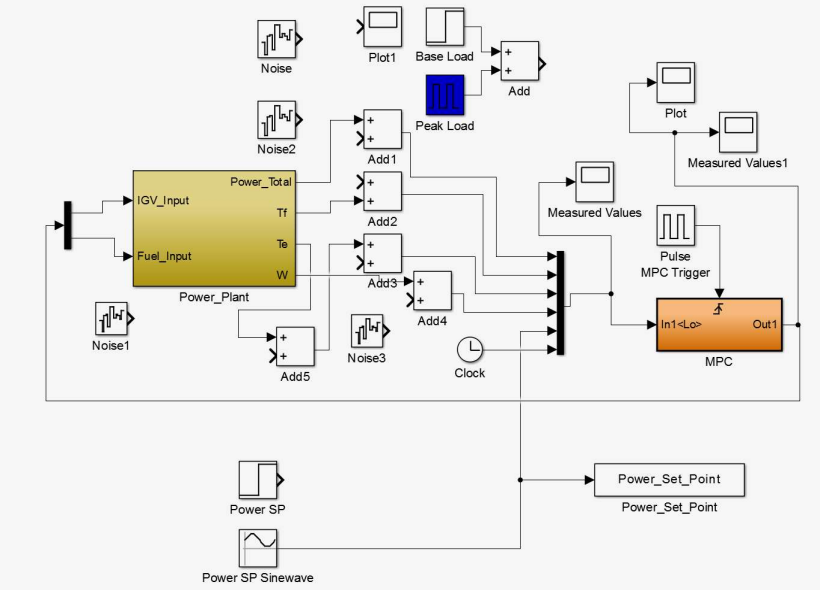

Figure 2: Power plant model with MPC

Results of Optimization

The power plant model currently runs a feedback system on the amount of power that needs to be generated. The power setpoint is fed into the controller and the controller sends a decision to the plant every 5 minutes. Initially, this led the plant to overpower then underpower the plant because the setpoint was continually changing. To combat the plant from being underpowered, the power deadband has a high penalty on going below the power setpoint.

Sensitivity Analysis

A sensitivity analysis shown below shows the effect of the manipulated variables (MV's) on the control variables (CV's). A change in IGV angle decreases the objective function, decreases both the exhaust and firing temperature, and slightly increases the total power output. The fuel flow rate decreases the objective function, increases the exhaust temperature, firing temperature and greatly increases the total power output. The effects of the MV's on the CV's are displayed below (Table XX)

Table 1: Sensitivity analysis of the system

Unit Increase in MVs	Objective Function	Exhaust Temperature (K)	Total Power (MW)	Firing Temperature (K)
IGV Angle	-61.9	-1.38	0.34	-1.3
Fuel Flow Rate	-4789.7	42.4	26.6	75.0

One of the initial problems with the controller was the system not being controlled to meet the power requirements. This was due to the controller not increasing fuel flow when more power was necessary. To combat this, the model in the model predictive control adds a fraction of the fuel onto the total power equation. This tells the model that fuel flow increases the output power. Results from the simulation are shown below. The total power has a moving set point being fed into the controller. The power plant has lower temperature initializations, so the power initially drops before the controller responds and brings the power up to the set point. The reason the power drops is that the compressor takes power to run. Initially the compressor energy demands are high compared to the overall power produced. Following initialization, the controller does well at following the set point throughout the simulation. The simulation runs for three days with a varying solar flux and varying power setpoint. Airflow rate is maximized throughout that time, and fuel flow is minimized.

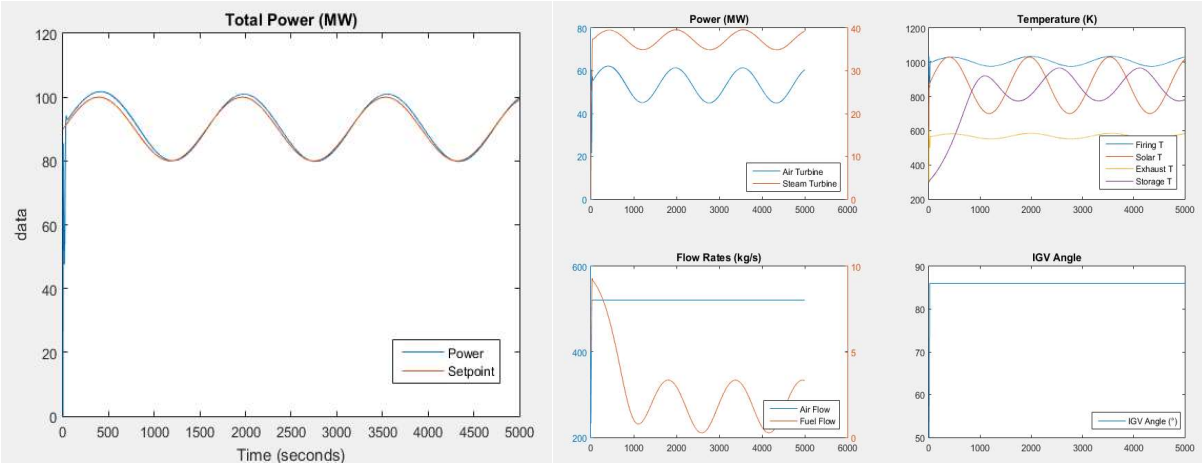

Figure 4: Simulation over a 3 day time horizon

Next, the benefits of solar storage are simulated. This was done by keeping solar radiation on and reducing the heat capacity of the solar storage system. In this manner, the storage system would have a more pronounced effect over shorter time horizons.

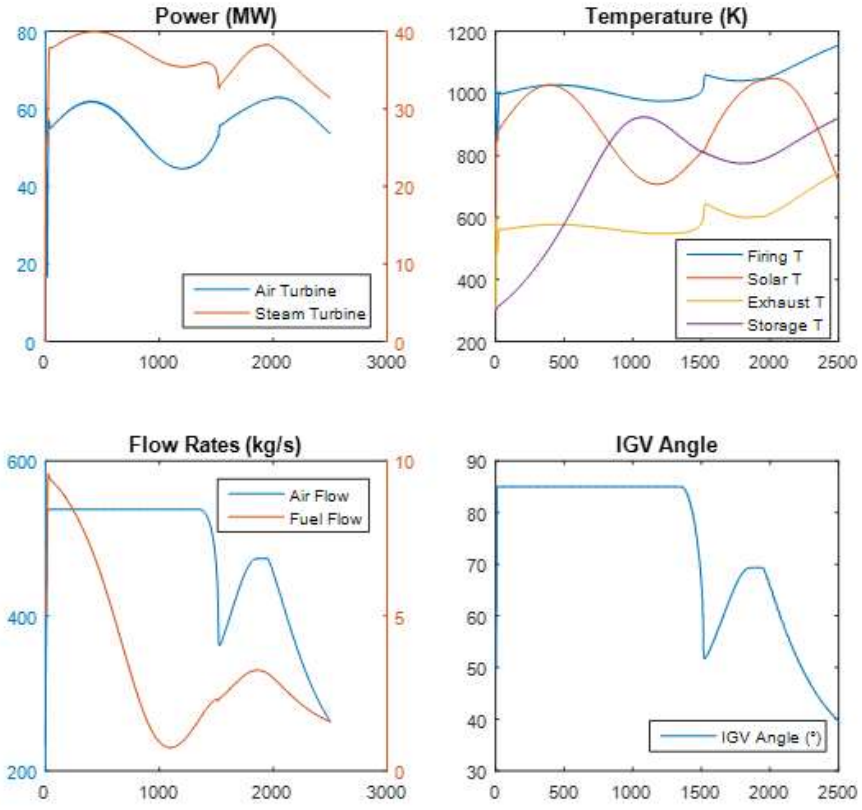

Figure 3: Simulation of power plant with solar radiation

The model is able to solve well over the shorter time horizon. The power set point is met throughout the time horizon. The discretized temperature segments of the solar radiation are also displayed below. The solar radiation initially heats up the stones. As the solar radiation decreases, the air passing through then takes energy from the stones and is heated.

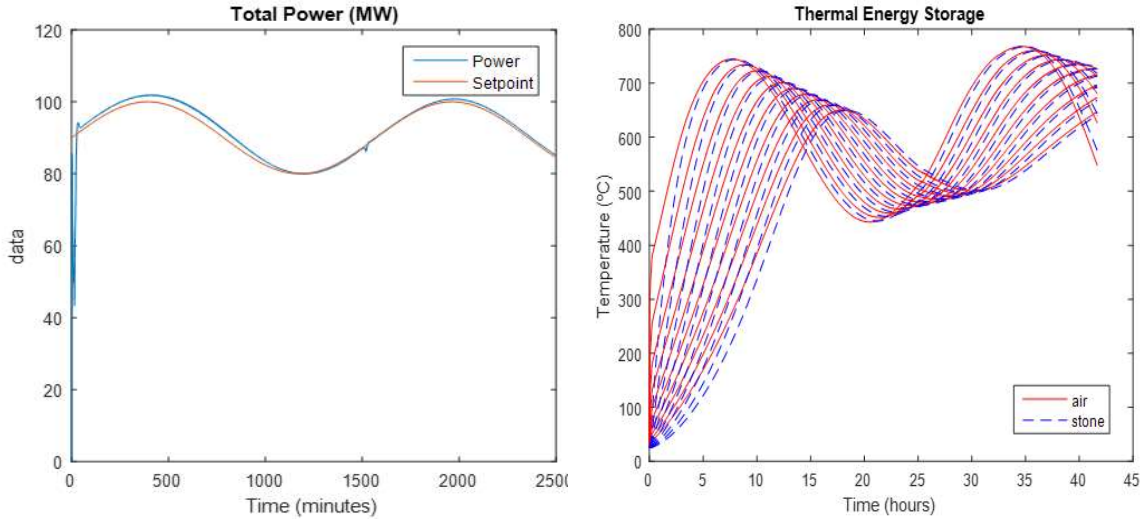

Figure 5: Power set point tracking with solar radiation and thermal energy storage

The next simulation shows no solar radiation. The air flow rate stays high since it is not taking in any energy from the solar arrays, and the fuel starts high, to meet the initial power and then begins to tail off. The controller is able to track the power setpoint throughout the run. The discretized solar storage source initially goes up to a steady state temperature, but remains there the entire time.

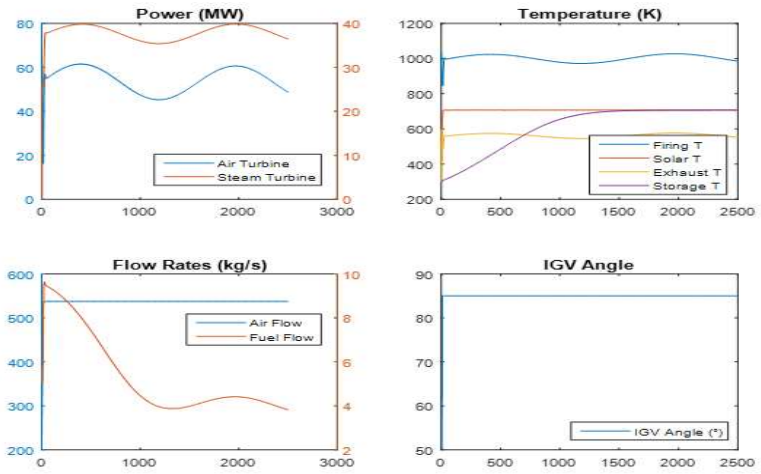

Figure 6: Simulation of power plant without solar radiation

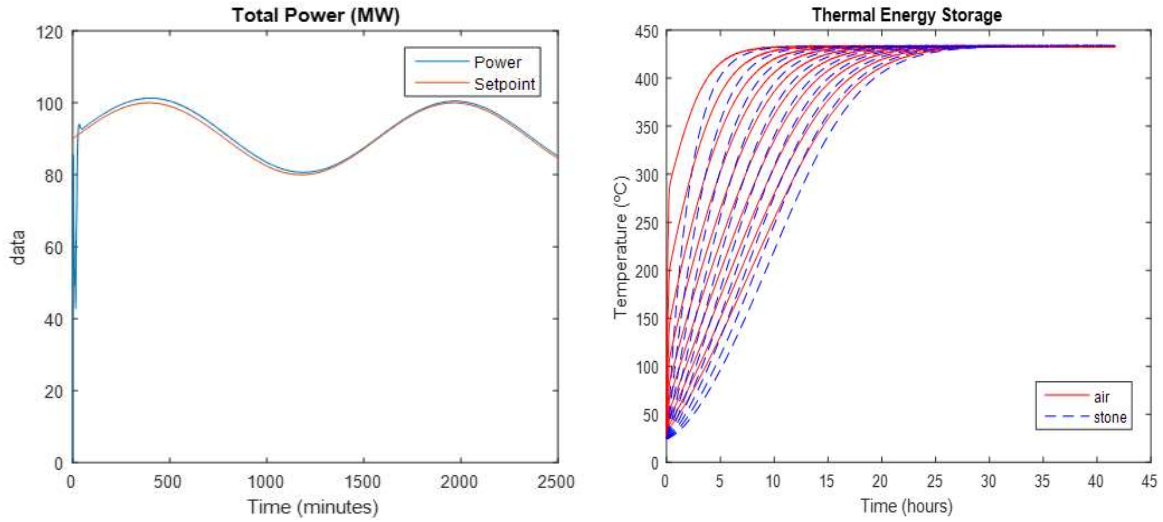

Figure 7: Power set point tracking without solar radiation and thermal energy storage

Discussion

Currently, the controller solves one timestep into the future to optimize the simulation. The purpose of simulating the controller with solar radiation and without solar radiation is to determine what effect the addition of solar radiation and energy storage has on the system. The first simulation is shown with solar radiation. As can be seen, the temperature of the storage system varies as the solar radiation goes up and down. The second simulation does not have solar radiation. The temperature of the storage reaches a setpoint and stays there. Both are able to reach the power setpoint, but each simulation completes the task in a different manner.

One way to increase the optimization would be to use a feedforward system feeding the power setpoints and the predicted solar radiation output into the controller. If this were done, the controller outputs would be able to be predicted in advance to optimize the system over the entire time horizon.

Conclusion

Controlling a hybrid power system is feasible using model predictive control. The system is able to meet the simulated energy demand, while minimizing fuel usage. The solar energy storage system is utilized by the simulator and helps smooth out disturbances in solar radiation. The current simulation fails to solve with some disturbances. Challenges of finding feasible solutions and solutions of how to overcome these challenges are found in the future work.

Future Work

The work presented in this report shows great promise for a hybrid power generation system, in theory, but as with many "green" endeavors, the ultimate setback of the project is the cost. The fact that it hybridizes with a cheap and abundant source of power generation (natural gas) suggests that it will be more economically viable than attempts to design energy generation systems that are wholly dependent on solar energy. Once a more detailed design on the hybrid system in this report is completed, an economic analysis would be necessary to determine the financial feasibility of a project such as this.

Some of the work that needs to be completed prior to the economic analysis are:

- Decrease model mismatch
- Increasing the model and solver robustness
- Creating a feedforward csv file for the weather and power demand
- Fully utilize the thermal storage with a bypass valve

One of the current issues with the simulation and the model is that there is mismatch between the two. One of the main reasons for this is in the initialization step. If the simulation and the model are not initialized at the same value, this results in model mismatch. To reduce or eliminate model mismatch, the simulation needs to feed back to the controller all temperature values. This would allow changes in the simulation to be reflected in the model.

Currently, changes in model inputs lead to problems with the model solving. The solver needs to be able to work with these disturbances and still solve. Many of these disturbances are easily measured or known in advance. To combat these disturbances, a combined feedforward

feedback system. This would allow the solver to detect the disturbances, and more easily converge to a solution. By feeding in weather and power demand curves, the optimizer could potentially come up with better solutions to meeting the power demand and minimizing fuel usage.

Finally, to fully utilize the feedforward and feedback system, there needs to be a bypass valve for the storage (Figure XXX). This would introduce an extra degree of freedom to the system. The extra degree of freedom would allow the air to store or obtain energy from the storage bed, or bypass the bed depending on what the future weather forecast is.

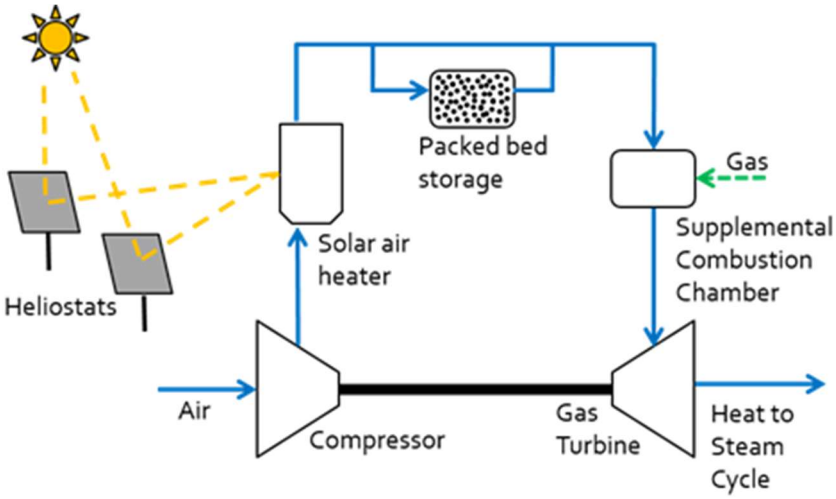

Figure 8: Future manipulated variable bypassing storage

References

[1] Kim, Jong Soo, Kody M. Powell, and Thomas F. Edgar. "Nonlinear model predictive control for a heavy-duty gas turbine power plant." American Control Conference (ACC), 2013. IEEE, 2013.

[2] Powell, Kody M., John D. Hedengren, and Thomas F. Edgar. "Dynamic optimization of a solar thermal energy storage system over a 24 hour period using weather forecasts." American Control Conference (ACC), 2013. IEEE, 2013.

[3] Powell, Kody M., and Thomas F. Edgar. "Modeling and control of a solar thermal power plant with thermal energy storage." Chemical Engineering Science 71 (2012): 138-145.

[4] Cole, Wesley J., Kody M. Powell, and Thomas F. Edgar. "Optimization and advanced control of thermal energy storage systems." (2012): 81-99.

[5] Powell, Kody M., and Thomas F. Edgar. "An adaptive-grid model for dynamic simulation of thermocline thermal energy storage systems." Energy conversion and management 76 (2013): 865-873.

[6] Adeyanju, A. A., and K. Manohar. "Theoretical and experimental investigation of heat transfer in packed beds." Research Journal of Applied Sciences 4.5 (2009): 166-177.

Appendix

Simulink Model

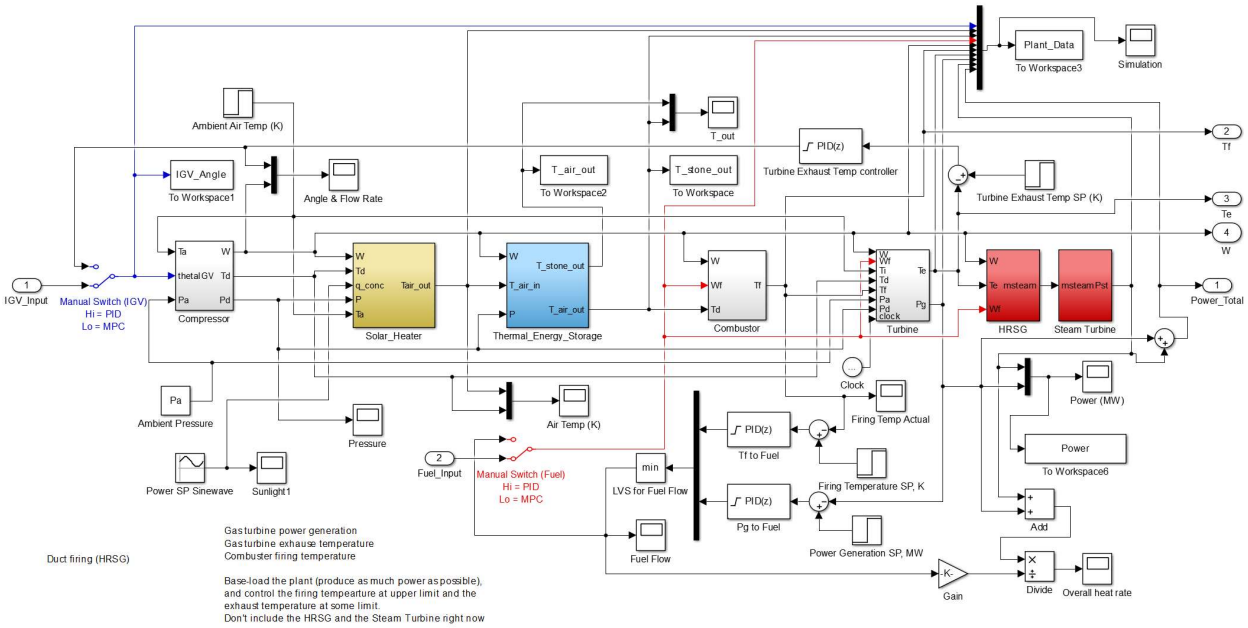

Constants and Parameters for Model Initialization

% Thermal Energy Storage (TES) Details

n_tes = 10; % number of TES nodes

R2 = 0.08206; % L-atm/mol-K % Could pull in through function

T_ref = 298; % K

k_stone = 1.7; % W/m-K

k_air = ones(n_tes,1); % W/m-K

h = ones(n_tes,1);

Nu = ones(n_tes,1);

```
Pr = ones(n_tes,1);
Re = ones(n_tes,1);
Vol_air = ones(n_tes,1);
v_air = ones(n_tes,1);
rho_stone = 2403;                % kg/m^3
sigma = 5.67e-8;                 % W/m2-K4 (Stefan-Boltzmann constant)
epsilon = 0.96;                  % emissivity of cement, red (200??C)
D = 5;                % m, tank diameter
len = 10;             % m, tank length
dp = 0.15;            % sphere diameter (m)
pi = 3.1415926;                          % pi
pct = 0.7;            % pct stone in tank (density)
A_tank = pi * D^2 / 4;           % Cross-sectional area of tank (m^2)
V_tank = A_tank * len;  % Volume of tank (m^3)
Ac = pct * A_tank;               % Cross sectional area of stone (m^2)
SA = 137.445;                    % Surface area of stone / slice (m^2)
x = len / n_tes;              % Discretization width (m)
A_air = (1 - pct) * A_tank;     % Cross-sectional area that air passes through (m^2)
Convection = 0;
Conduction = 0;
Radiation = 0;

% W = 475/60; % (kg/min)
% GD = W / A_air / dp * 2.204621 / 3.28084^3 * 3600; % lb/hr-ft3
% h = 0.652 * GD^0.7 * 0.29307 * 3.28084^3 / 1.8; % W/m3-K
% h = 12 ...
```

```
T_stone0 = ones(n_tes,1)*298;   %K, TES stone node initial conditions

T_air0 = ones(n_tes,1)*298;     %K, TES air node initial conditions

q_cond = zeros(n_tes,1);

q_conv = zeros(n_tes,1);

q_rad = zeros(n_tes,1);

Cp_air = ones(n_tes,1)*300;

Cp_stone = ones(n_tes,1)*1584;

rho_air = zeros(n_tes,1);

mu_air2 = zeros(n_tes,1);

m_air = zeros(n_tes,1);

m_stone = ones(n_tes,1) * V_tank * rho_stone * pct / n_tes;          % Mass of stone in each slice (kg)

flag = 0; % For plot axis resizing purposes

C = [2.8958e04; 9.3900e03; 3.0120e03; 7.5800e03; 1.4840e03]; % Heat capacity of air

B = [-0.22824; 3.3801e5; -3.4738e7; 110.88; -2378.1]; % Heat capacity of stone (granite)

E = [3.1417E-04; 7.7860E-01; -7.1160E-01; 2.1217E+03]; % Air thermal conductivity

F = [1.4250E-06; 5.0390E-01; 1.0830E+02; 0]; % Viscosity of air (kg/m/s = Pa*s)


%External heat loss (TES)

wall_1 = 0.05; % m (steel wall thickness)

wall_2 = 0.15; % m (insulation thickness)

wall_3 = 0.01; % m (outer metal thickness)

thick = 0.21; % m (TES wall total thickness)

A_inner = 2 * pi * (D / 2) * len / n_tes; % Inner surface area

A_outer = 2 * pi * (D / 2 + thick) * len / n_tes; % Outer surface area

A_lm = (A_outer - A_inner) / log(A_outer / A_inner); % Log mean surface area

T_wall_inner = ones(n_tes,1)*298;
```

```
T_wall_outer = ones(n_tes,1)*298;
U_wall = 0.1; % W/m2-K (heat loss through TES wall)
q_external = zeros(n_tes,1); % Heat loss through tank wall

% receiver details
R = 8.314; %m^3*kPa/kmol*K
MW_air = 28.97; %kg/kmol
sig = 5.6704e-11; %kW/(m^2*K^4), Stefan-Boltzmann constant
mu_air = 1.983e-5; %kg/(m*s), absolute viscosity of air at 300K
emiss_rec = 0.1; %receiver emissivity
h_node_rec = 2; %m, receiver node height
n_rec = 10; %number of receiver nodes
U = .010; % kW/m^2K
w_rec = 10; % m, width of receiver
d_rec = 5; %m, depth of receiver
Trec0 = ones(n_rec,1)*550; %K, receiver node initial condition

eta_c = 0.86;
eta_comb = 0.99;
Cpc = 1.005; %kJ/kg*K, heat capacity of air (cold)
Cph = 1.157; %kJ/kg*K, heat capacity of air (hot)
gamma_c = 1.4;
gamma_h = 1.33;
eta_t = 0.89;
Wn = 537; %kg/s, nominal air flow
Wfn = 10.2; %kg/s, nominal fuel flow
LHV = 46000; %(kJ/kg) LHV of natural gas - not from paper -
```

```
%http://www.engineeringtoolbox.com/heating-values-fuel-gases-d_823.html
PR = 15.4; %compressor pressure ratio
Ta0 = 288.15; %ambient temp, K
Pa0 = 101.325; %kPa
theta0 = 11.6; %reference IGV angle in degrees
thetaMAX = 85; %maximum IGV angle
A0 = .945; A1 = -7.8; A2 = 39;

T = 0.05; %speed governor time constant
Ti = 18.5;
Tw = .4789; %Air control time constant
Kf = 0; % Fuel system ext. feedback const.
Tv = 0.04; %Valve positioner time constant
K6 = 0.1062; %fuel valve lower limit
T5 = 0.5;
Tt = 100;
Tf = 0.26; %fuel system time constant
T6 = 60; %Time constant of Tf control
T4 = 1.7; %thermocouple time constant
K4 = 0.85; %gain of rad shield
T3 = 12.2; % Rad shield time constant
K5 = 0.15; %Gain of rad. shield
K3 = .8938; %Ratio of fuel adjustment
Tg = 0.05;
Tcd = .16;

PI = 160;
```

```
TI = 298;
Pa = 101.325; %kPa

Hsh = 3231; %kJ/kg, superheated steam enthalpy at 30 bar and 400 C
Hsv = 2809; %kJ/kg, saturated vapor enthalpy at 30 bar and 233.8 C
%(http://www.engineeringtoolbox.com/enthalpy-superheated-steam-d_1130.html)
Hfg = 1793.94; %kJ/kg, heat of vaporization at 30 bar
%(http://www.engineeringtoolbox.com/saturated-steam-properties-d_457.html)
Cpw = 4.78; %kJ/kgK, Cp of liquid water
delTbfw = 120; %k, delta H of boiler feed water (assume makeup water mixes...
%with saturated liquid to bring temp down by this much

dHtot = (Hsh-Hsv)+Hfg+Cpw*delTbfw; %kJ/kg, total water to steam specific
%enthalpy

Hsv1bar = 2676; %specific enthalphy of sat steam at 1 bar
%http://www.engineeringtoolbox.com/saturated-steam-properties-d_101.html

Tao = 450; %exhaust air outlet temp
eta_HRSG = 0.95; %HRSG efficiency

Hliq = 350.6; %kJ/kg, condensed liquid enthalpy (@0.55 bar)
xsat = 0.9; %percent saturation
Hfg = 2299; %kJ/kg, heat of vaporization at 0.55 bar
%from http://www.engineeringtoolbox.com/saturated-steam-properties-d_101.html
Hcond = Hliq + xsat*Hfg; %total enthalpy of condensed state at 0.55 bar
```

```
dHst = Hsh - Hcond; %kJ/kg, delta H for steam turbine

eta_st = 0.95; %efficiency of steam turbine/generator

%% solar receiver model parameters
```